Lab on a Chip

Dynamic Article Links

Cite this: *Lab Chip*, 2011, **11**, 3465

www.rsc.org/loc

PAPER

An integrated passive micromixer–magnetic separation–capillary electrophoresis microdevice for rapid and multiplex pathogen detection at the single-cell level†

Jae Hwan Jung, Gha-Young Kim and Tae Seok Seo*

Received 26th April 2011, Accepted 15th July 2011
DOI: 10.1039/c1lc20350a

Here we report an integrated microdevice consisting of an efficient passive mixer, a magnetic separation chamber, and a capillary electrophoretic microchannel in which DNA barcode assay, target pathogen separation, and barcode DNA capillary electrophoretic analysis were performed sequentially within 30 min for multiplex pathogen detection at the single-cell level. The intestine-shaped serpentine 3D micromixer provides a high mixing rate to generate magnetic particle–pathogenic bacteria–DNA barcode labelled AuNP complexes quantitatively. After magnetic separation and purification of those complexes, the barcode DNA strands were released and analyzed by the microfluidic capillary electrophoresis within 5 min. The size of the barcode DNA strand was controlled depending on the target bacteria (*Staphylococcus aureus*, *Escherichia coli* O157:H7, and *Salmonella typhimurium*), and the different elution time of the barcode DNA peak in the electropherogram allows us to recognize the target pathogen with ease in the monoplex as well as in the multiplex analysis. In addition, the quantity of the DNA barcode strand ($\sim 10^4$) per AuNP is enough to be observed in the laser-induced confocal fluorescence detector, thereby making single-cell analysis possible. This novel integrated microdevice enables us to perform rapid, sensitive, and multiplex pathogen detection with sample-in-answer-out capability to be applied for biosafety testing, environmental screening, and clinical trials.

Introduction

Laboratory-on-a-chip (LOC) technology has continuously progressed by incorporating several chemical and biological functional units into a single wafer. Microfluidics-based miniaturization and integration provides a number of advantages such as fast analytical time, reduced sample consumption, high detection sensitivity, automation, and portability.[1–4] Current research directions move toward embedding a sample preparation step on-chip to realize a fully integrated LOC for point-of-care (POC) testing. Applications of LOC in the fields of biological diagnostics and high-throughput bio/chemical-screening have been demonstrated, and pathogen analysis on a chip has particularly attracted attention due to the dramatically increased threat of infectious disease for the public.[5,6] Therefore, the on-site rapid and accurate pathogen diagnostics are demanded, and for this purpose, research efforts have focused on incorporating various molecular assays such as polymerase chain reaction (PCR), microarray, or enzyme-linked immune-sorbent assay (ELISA) into the microfluidic platforms.[7–14]

Liu *et al.*[7] reported a fully integrated biochip device consisting of magnetic bead based sample preparation, PCR, and DNA microarray for electrochemical detection of *E. coli* K12 bacteria and single nucleotide polymorphism. Lagally *et al.*[8] presented a portable system integrating PCR and capillary electrophoresis (CE) capable of detecting as few as 2–3 *E. coli* cells, and Beyor *et al.*[9] have further implemented a cell capture device into the PCR-CE microdevice for *E. coli* O157 detection with a detection limit of 0.2 CFU μL^{-1}. Although the PCR based genetic analytical microdevice provides high sensitivity by amplifying the number of target genes, there are limitations in terms of the complicated fabrication process, high cost, complex instrumentation, and prolonged assay time. Herrmann *et al.*[13] and Yu *et al.*[14] have demonstrated a microfluidic ELISA system for identifying anti-streptavidin antibodies and biomarkers based on the convenient colorimetric detection. However, the integration of sample pretreatment unit and the reduction of assay time are still needed,[15,16] and the detection sensitivity should be improved considering that the infectious dose of pathogens such as *E. coli* O157 is as low as 1 CFU.[17] Thus, an advanced integrated

Department of Chemical and Biomolecular Engineering (BK21 program) and Institute for the BioCentury, Korea Advanced Institute of Science and Technology (KAIST), 291 Daehak-ro, Yuseong-gu, Daejeon, 305-701, South Korea. E-mail: seots@kaist.ac.kr; Fax: +82 42 350 3910; Tel: +82 42 350 3933

† Electronic supplementary information (ESI) available: Information on optimum amount of antibody for the conjugation with AuNP probes (Fig. S1) and electropherogram of monoplex pathogen detection (Fig. S2). See DOI: 10.1039/c1lc20350a

microdevice with more simplified design, rapid bioassay reaction, and highly sensitive and multiplex detection is required for point-of-care pathogen detection systems.

Recently, the nanoparticle based DNA barcode assay has demonstrated its ability for detecting target proteins or nucleic acids with ultrahigh sensitivity.[18–26] This barcode assay uses two types of particle probes: magnetic microparticle (MMP) with recognition elements for the target of interest and gold nanoparticle (AuNP) with a second recognition agent and thiolated barcode DNAs. After reaction of particle probes with the analytes, the sandwich structured immuno-complexes (*i.e.*, MMP-target-AuNP) are isolated by magnetic separation, followed by dehybridization of the barcode DNA from the NP probes. The released barcode DNAs are analyzed by several methods, such as microarray *via* scanometric detection,[18–22] colorimetric detection using a thin-layer chromatography plate,[23] a capillary DNA analyzer,[24] electrochemical detection,[25] and fluorescence detection,[26] which indirectly identify the presence of target molecules. Although the subsequent barcode DNA detection method can increase the detection sensitivity up to attomolar concentration, the process was generally performed manually and required another set of DNA arrays to capture the barcode DNA which consumes the assay time and extra cost. Among the nucleic acid detection methods, CE on a microchip provides more precise, simple, rapid, and quantitative analysis over the DNA hybridization method. Size-dependent elution time of peaks in the electropherogram enables us to recognize the target DNA with ease, and the single base resolution separation on a chip makes it possible to analyze the multiplex DNA molecules.[19] Due to these advantages, the micro-CE based genetic analysis is widely applied for short tandem repeat genotyping,[10] DNA sequencing,[11] and single nucleotide polymorphism analysis.[12]

In this study, we have integrated a microdevice for the DNA barcode assay with a CE microfluidic system for multiplex pathogen detection. For the DNA barcode assay, a novel efficient passive mixer and a magnetic separation chamber were developed which are connected with a CE microchannel with a cross-injector design. Monoplex as well as multiplex detection of three target pathogens (*i.e.*, *Staphylococcus aureus*, *Escherichia coli* O157:H7, and *Salmonella typhimurium*) were successfully demonstrated on an integrated passive micromixer–magnetic separation–capillary electrophoresis (PMMS-CE) microdevice. The laser-induced fluorescence detection on a CE channel proves its ability of highly sensitive DNA analysis by showing single-cell pathogen detection. Such a fully integrated DNA barcode assay microdevice provides fast, sensitive, and multiplex pathogen identification with a sample-in-answer-out capability which is applied for point-of-care testing of disease diagnostics.

Experimental

Antigens, antibodies, and barcode DNAs

The three target bacterial cells (*i.e.*, *Staphylococcus aureus* (KCTC 1621), *E. coli* O157:H7 (KCTC 1039), and *Salmonella typhimurium* (KCTC 2054)) were purchased from Korean Collection for Type Cultures (KCTC). Those were grown aerobically in a nutrient agar (beef extract 3 g, peptone 5 g, agar 15 g, distilled water 1 L) at 37 °C. The mouse monoclonal antibodies of *Staphylococcus aureus* and *E. coli* were purchased from Millipore (Temecula, CA, USA) and those of *Salmonella typhimurium* were from Santa Cruz Biotechnology (Santa Cruz, CA, USA). Three pairs of thiolated and FAM-labeled barcode DNA strands were used to synthesize the AuNP probes. The sequences of barcode DNA strands are as follows: 5′-SH-C_6-GGTAAG-CATCGAGGTAAGCA-3′ and 5′-FAM-TGCTTAC-CTCGA-TGCTTACC-3′ (20-mer) for *Staphylococcus aureus*; 5′-SH-C_6-AAAAAAAAAAAAAAATACCACATCATCCAT-3′ and 5′-FAM-ATGGATGATGTGGTATTTTTTTTTTTTTTT-3′ (30-mer) for *E. coli* O157:H7; 5′-SH-C_6-AAAAAAAAAAAAAAA-TACCTACTACAAAATAAAAAAAAAA-3′ and 5′-FAM-TT-TTTTTTTTATTTTGTAGTAGGTATTTTTTTTTTTTTTT-3′ (40-mer) for *Salmonella typhimurium*.

Preparation of particle probes

The particle probes were synthesized according to the previously published protocols.[18–20] Tosyl-activated magnetic beads (Dynabeads® M280 Tosyl-activated, dia. = 2.8 μm, Invitrogen, Carlsbad, CA, USA) were covalently linked to the primary amino groups of antibody. 100 μL of MMPs (~2×10^8) was washed three times with 1 mL of borate buffer (0.1 M, pH 9.5) in conjunction with magnetic separation and re-suspended in 200 μL of borate buffer containing 60 μg of antibody (Ab) (3 μg antibody per 10^7 MMPs). The conjugation of MMPs with Ab was carried out at 37 °C for 24 h under vortex. Then, the Ab-conjugated MMPs were placed on a magnet and washed with PBS (0.01 M, pH 7.4) for 5 min at 4 °C. Subsequently, the MMP probes were passivated by adding 250 μL of blocking buffer (0.2 M Tris, pH 8.5) for 4 h at 37 °C and washed for 5 min at 4 °C. The synthesized MMP probes were stored in 1 mL of PBS at 4 °C prior to use. The coupling efficiency was measured based on the absorbance at 280 nm before and after the reaction (coupling efficiency (%) = $\{(A_{280,\text{before}} - A_{280,\text{after}})/(A_{280,\text{before}})\} \times 100$). The loaded amount of each Ab in 2×10^8 MMPs was calculated as 50.9 μg for monoclonal anti-*Staphylococcus aureus*, 56.4 μg for monoclonal anti-*E. coli* O157:H7, and 34.4 μg for monoclonal anti-*Salmonella typhimurium* with the coupling efficiency of 84.8, 93.9, and 57.1%, respectively. The gold nanoparticle (AuNP) probes were prepared by adding Ab to 0.1 mL of AuNP solution (2×10^{11} mL^{-1} ≈ 330 fmoles mL^{-1}, dia. = 30 nm, BBInternational, UK) at pH 9.2. The amount of each Ab for the conjugation with AuNPs was roughly estimated as 100 ng for *Staphylococcus aureus*, 300 ng for *E. coli* O157:H7, and 100 ng for *Salmonella typhimurium* with 2×10^{10} AuNPs (Fig. S1†).[20]

After incubation for 30 min at room temperature under slow vortex by using a Dynabeads® Sample Mixer, the Ab modified AuNPs were reacted with the freshly cleaved thiolated barcode DNA strands (1 nmole) for 16 h. The thiolated barcode DNAs were prepared by reducing the protecting disulfide bond to thiol group by treatment with dithiothreitol (DTT, Sigma-Aldrich, MO, USA) and purified through illustra NAP-5 columns (GE Healthcare, NJ, USA). Next, the AuNPs were salt-stabilized with 0.1 M NaCl and passivated with 1% BSA solution for 30 min. The AuNPs were centrifuged at 13 000 rpm for 1 h at 4 °C and the supernatant was removed, and this washing step was repeated twice. Subsequently, the AuNPs were re-suspended in PBS and then hybridized with the FAM-labelled complementary

barcode DNA strands for 6 h at 37 °C. The Ab and duplex barcode DNA labelled AuNPs were again purified using the centrifugation procedure and re-dispersed in 200 μL of washing buffer (*i.e.*, PBS containing 0.1% BSA and 0.02% Tween 20). The prepared AuNP probes were stored at 4 °C prior to use. The loading amount of DNA was determined based on the absorbance at 260 nm. The numbers of barcode DNA complements per 2×10^{10} AuNP probes were 0.368, 0.377, and 0.434 nmoles, which correspond to 1.11×10^4, 1.13×10^4, and 1.31×10^4 barcode DNA strands per each AuNP, respectively.

Design and fabrication of a microdevice

The design of the PMMS-CE microdevice is presented in Fig. 1 which is composed of three parts: a passive mixer, a magnetic separation chamber, and a capillary electrophoretic microchannel. The passive mixer has an intestine-shaped serpentine 3D structure to create an effective mixing and an immuno-binding reaction. It has dimensions of 17.9 cm length × 250 μm width × 100 μm height and a total volume of 3.80 μL. The magnetic separation chamber which has a volume of 1.8 μL is sandwiched between an external magnet on the top and a film heater underneath. The barcode DNA plug generated in the separation chamber travels down a CE channel with a 6 cm separation length which incorporates a cross-injector design.

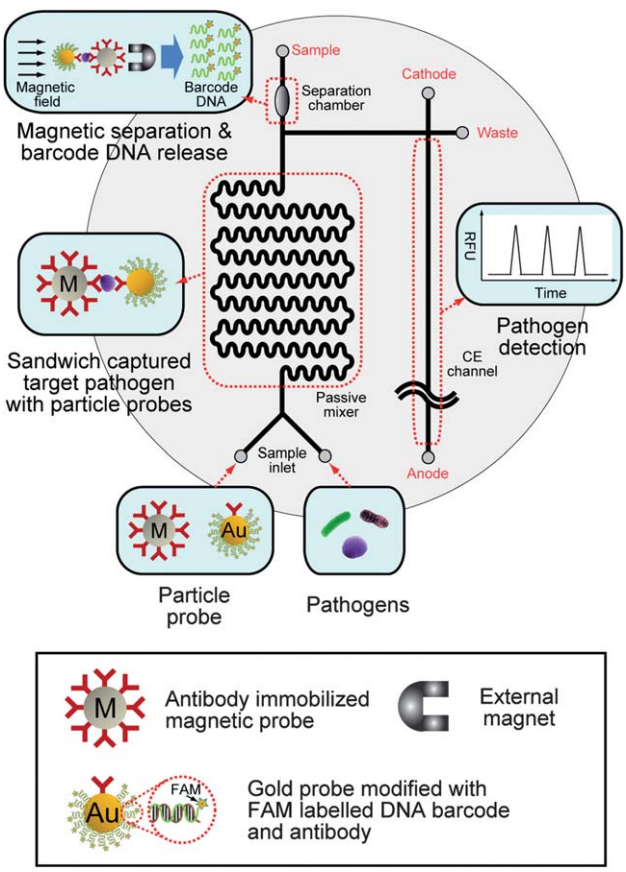

Fig. 1 Schematic diagram of an integrated PMMS-CE microdevice which performs a DNA barcode assay and a capillary electrophoretic separation for multiplex pathogen detection. The PMMS-CE microdevice consists of a passive mixer for target capture with particle probes, a magnetic separation chamber for isolating and purifying the target complexes, and a capillary electrophoretic microchannel for detecting barcode DNA strands to identify target pathogens.

The passive mixer integrated PMMS-CE microdevice is made of a glass–glass wafer. To form the passive mixer–separation chamber–CE channel pattern on the upper wafer, a 100 mm borofloat wafer (1.1 mm thickness, PG&O, Santa Ana, CA, USA) was coated with 200 nm amorphous silicon using low-pressure chemical vapor deposition. The photoresist (S1818, Rohm & Haas, Philadelphia, PA, USA) was spin-coated with 2 μm thickness, and the passive mixer–separation chamber–CE channel pattern of the mask was transferred by UV exposure. After developing, the exposed Si hard mask was removed by reactive ion etching (RIE) in SF_6 plasma (VSRIE-400A, Vacuum Science, Korea). Isotropic wet etching was followed in 49% hydrofluoric acid solution for 8 min to achieve a depth of 50 μm and a width of 140 μm. The remaining photoresist was cleaned in acetone for 10 min, and the sacrificial silicon layer was then removed by RIE in SF_6 plasma. Reservoir holes were drilled with 1 mm diameter on a Sherline vertical milling machine (Model 2010, Sherline Products, Vista, CA, USA). The intestine-shaped serpentine passive mixer structure was also fabricated on the bottom wafer following the above process with 50 μm depth, and then the two wafers were aligned and thermally bonded at 668 °C for 2 h. A 3 mm diameter punctuated PDMS membrane (3 mm thickness) was treated in a UV-ozone cleaner for 5 min, and then assembled on the sample, cathode, waste, and anode reservoirs for electrode connection.

Operation of the PMMS-CE microdevice

The procedure of the PMMS-CE microdevice for pathogen detection is divided into two steps: target pathogen capture and barcode DNA detection by CE. Those steps on a microdevice are illustrated in Fig. 1. First, the CE microchannel was cleaned with 1 M NaOH and 1 M HCl for 10 and 3 min respectively and rinsed with water. Then, the channel was pretreated with 50% v/v dynamic coating in methanol (DEH-100, The Gel Company, San Francisco, CA, USA) for 2 min to minimize electroosmotic flow during separation. The separation channel was filled with a 5% linear polyacrylamide (LPA) with 6 M urea from the anode reservoir as a sieving matrix. The waste, cathode, and anode reservoirs were occupied with 1× TTE (Tris TAPS EDTA) buffer. Next, the aqueous solution of MMP and AuNP probes (each 10 μL), and sample solution containing target pathogens (10 μL) were introduced into a microfluidic channel from the sample inlet by using a syringe pump. The solutions flowed and mixed well along with the passive mixer forming the sandwich immuno-complexes, magnetic particle–pathogenic bacteria–duplex DNA barcode labelled AuNPs. The immuno-complexes were collected on the separation chamber with a magnet while the unbound particle probes and targets were washed away with PBS (0.01 M, pH 7.4). The FAM-labelled barcode DNA strands were dehybridized from the NP probes by heating the chamber with a silicon rubber heater (SR020312, Hanil Electric Heat Engineering, Korea) at 95 °C for 3 min. Then, the high-voltage power supply was applied to move the FAM-labelled DNA to the CE separation channel. The CE operation and the laser-induced fluorescence detection were performed according to the previously published literature.[27–29] Briefly, the separation

channel was heated with a silicon rubber heater (SR020312, Hanil Electric Heat Engineering, Korea) and maintained at 70 °C which was monitored by a temperature controller (TZ4ST-14S, Autonics, Korea). 1000 and 0 V power supplies (PS300 series, Stanford Research Systems) were applied to the waste and sample reservoirs for 60 s to load the released barcode DNA strands into the injection channel. To isolate a DNA plug at the injection cross, 900 V was applied at the sample and waste reservoirs for 10 s with an electric field strength of 300 V cm^{-1} along the separation channel. Then, the CE separation was followed by applying 1800 V at the anode, while the sample and waste electrodes were floated. These series of CE operations were controlled automatically by a LabVIEW program.

The fluorescence emission signals of the separated FAM-labelled barcode DNA strands were detected by using a laser-induced confocal fluorescence microscope (C1si, Nikon, Japan). An excitation wavelength of 488 nm from an argon laser was used, and the power intensity measured from a 10× Plan Apo objective (NA 0.45) was 3.6 mW. The scanning area (0.016 mm^2) was defined on the separation channel near the anode reservoir, and data were obtained with a scanning rate of 5 frames per second. The emission signal of the FAM was detected through a band pass filter of 505–530 nm. The peaks in the electropherogram were quantified using the PeakFit (Version 4.12) software.

Results and discussion

Intestine-shaped serpentine 3D micromixer

To maximize the cell capture efficiency for generating sandwich-type immuno-complexes, magnetic microparticle–pathogenic bacteria–duplex DNA barcode labelled AuNPs, it is critical to optimize a micromixer and flow rate. A variety of passive micromixers have been reported so far,[30–33] and a serpentine design was widely employed because of the high and rapid mixing efficiency derived from the centrifugal force at the corners.[34] In addition to the serpentine design, we incorporated a regular tooth-shaped projection inside the serpentine microchannel to further enhance the mixing efficiency. Both the upper and lower glass wafers have such a tooth-shaped projection which is alternate after bonding as shown in Fig. 2(a) (bottom), so that the intestine-shaped serpentine 3D structures drive the pathogen sample and particle probe solutions horizontally as well as vertically, resulting in the improvement of the mixing efficiency and the formation of the immuno-complexes. To demonstrate the mixing efficiency of our novel passive mixer design, we performed a mixing test by using red and blue dyes in the intestine-shaped serpentine PDMS channel which has the same dimension as shown in Fig. 1. A full mixing of the passive mixer was achieved after passing 4 mixing units (approximately within a length of 3.25 cm, 25% of the total length) even at a high flow rate of 5000 μL h^{-1}, which was confirmed by observing uniform violet color in the magnified digital image. This result implies that a lower flow rate could produce better mixing performance. Therefore, we first evaluated the cell capture efficiency at various flow rates by controlling the retention time of particle probes and target cells in the passive mixer. A cell sample (10^5 CFU of *Staphylococcus aureus*) was injected with the particle probes and mixed along with the microfluidic channel at flow rates from 3.8 to 100 μL h^{-1}. The immuno-complexes were then isolated with a magnet placed on the top of the separation chamber, and then the barcode DNAs were released by heating the chamber with the use of a rubber heater. The fluorescence signal of the recovered barcode DNAs was quantitatively analyzed by CE, and the relative cell capture efficiency was obtained under the assumption that the fluorescence signal at 60 min of retention time, which corresponds to a flow rate of 3.8 μL, is 100%. Fig. 2(b) shows that the cell capture efficiency of the PMMS-CE chip increased in proportion to the retention time. In particular, 75% of cells were captured at a retention time of 20 min (*i.e.*, a flow rate of 11.5 μL h^{-1}). Although about 47% of relative cell capture efficiency was obtained in only 12 min, we fixed the retention time at 20 min for further experiments to conduct the whole process rapidly as well as to maintain high detection sensitivity for pathogen detection.

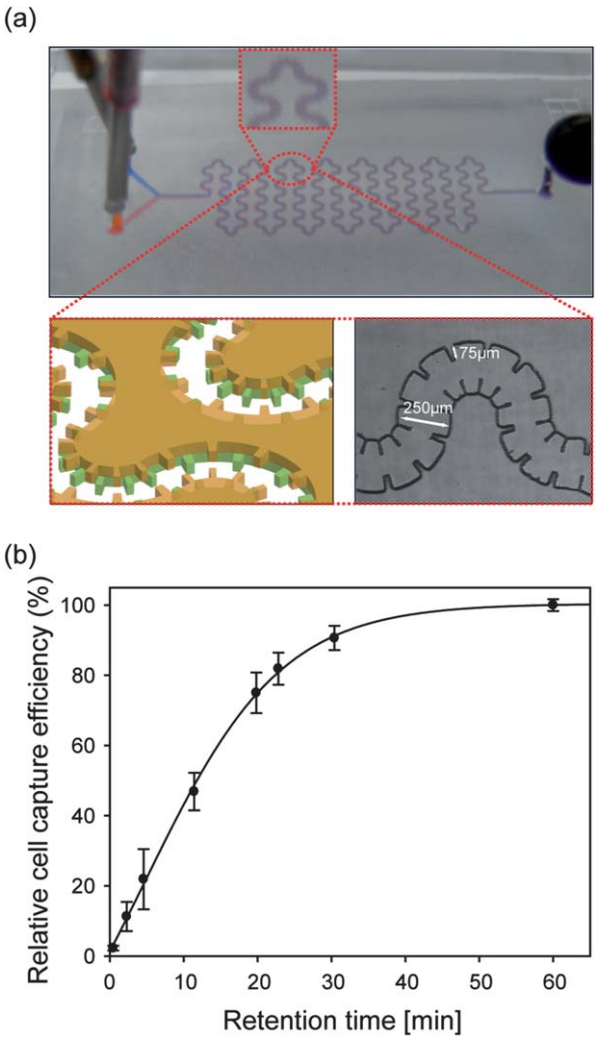

Fig. 2 (a) Mixing test of a novel intestine-shaped serpentine 3D passive mixer and (b) the effect of retention time on the cell capture efficiency with 10^5 CFU of *Staphylococcus aureus*.

Monoplex detection

To realize the potential of the PMMS-CE microdevice for quantitative and sensitive detection of pathogens, it is critical

that this novel device should provide good signal response over several orders of magnitude with low limit of detection (LOD). Thus, we demonstrated the ability of the PMMS-CE microdevice to identify the target pathogens in the range of 1–10^6 CFU for *Staphylococcus aureus*, *E. coli* O157:H7, and *Salmonella typhimurium*. Fig. S2† shows that the increased concentration of the target cell generated higher peak intensity in the electropherogram. The elution times of each peak were 160, 180, and 200 s which were matched with 20-mer barcode DNA for *Staphylococcus aureus*, 30-mer barcode DNA for *E. coli* O157:H7, and 40-mer barcode DNA for *Salmonella typhimurium*. Those fluorescence peaks of DNA barcode strands were produced in the electropherogram within 5 min, showing high speed of pathogen detection using the PMMS-CE microdevice. Fig. 3 shows the calibration curve of each pathogen by plotting the fluorescence peak intensity *versus* target cell concentration, revealing a sigmoidal relationship, and the dynamic range of each pathogen was determined as 1–10^6 CFU (Tables S1 and S2†). Importantly, the fluorescence intensity at 1 CFU of each pathogen (31 ± 4.8, 46 ± 6.2, and 11 ± 4.8 RFU for *Staphylococcus aureus*, *E. coli* O157:H7, and *Salmonella typhimurium*, respectively) was clearly distinguished from the background noise (1.92 ± 0.65 RFU), indicating single cell detection was successfully performed. Note that the total analysis time is less than 30 min (immuno-reaction: 20 min, magnetic separation and barcode DNA dehybridization: <5 min, CE separation and detection: <5 min).

Multiplex pathogen detection

To evaluate the selectivity and multiplexing capability for pathogen detection on the PMMS-CE microdevice, four tests were run with different combinations of the target pathogens where all three sets of particle probes were present. We systematically combined two types of targets (*Staphylococcus aureus* + *E. coli* O157:H7, *Staphylococcus aureus* + *Salmonella typhimurium*, and *E. coli* O157:H7 + *Salmonella typhimurium*) as well as all the three targets (*Staphylococcus aureus* + *E. coli* O157:H7 + *Salmonella typhimurium*) under the same conditions of the input cell number of 10^5 CFU. Fig. 4(a) represents the resultant electropherogram for multiplex pathogen detection in which all the peaks appeared at the elution time with high signal-to-noise ratio. Therefore, the presence of target pathogens was accurately determined, and importantly only target specific barcode oligonucleotides from the particle–pathogen immuno-complex were detected although all the particle probes coexisted, meaning no cross-immunobinding occurred between the particle probes and pathogens. The difference in the fluorescence signal intensities of each target bacterium is likely related to the different binding constants of the antigens with the corresponding antibodies.[19] Since the microfluidic CE analytical tool is widely adopted for DNA separation with good sensitivity and resolution, these results imply that we have much room for improvement in the multiplexing analysis in our PMMS-CE system by combining the

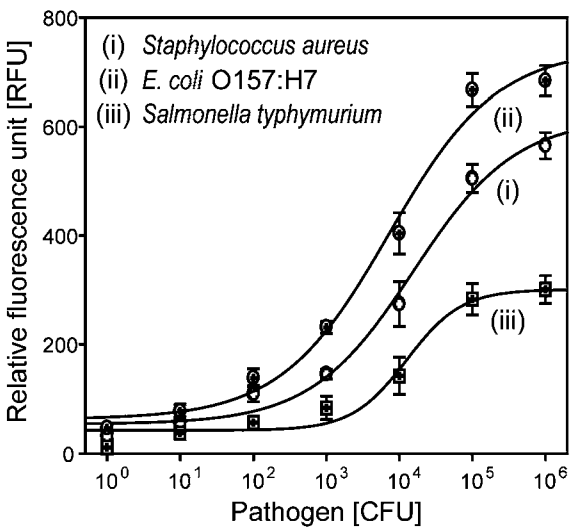

Fig. 3 Fluorescence measurements as a function of target pathogen concentration.

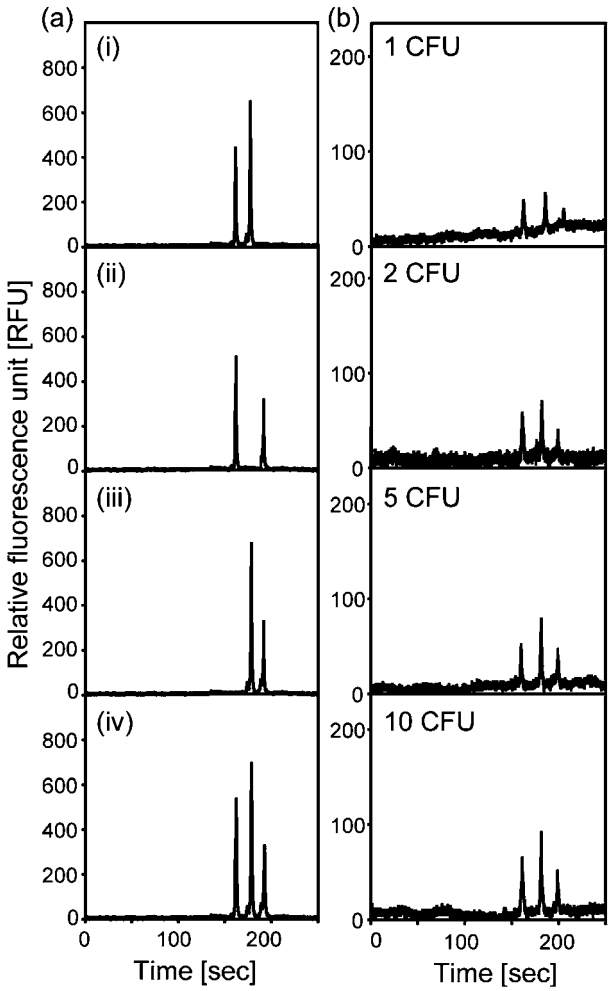

Fig. 4 (a) Multiplex detection of pathogens by using a PMMS-CE microdevice: (i) *Staphylococcus aureus* + *E. coli* O157:H7, (ii) *Staphylococcus aureus* + *Salmonella typhimurium*, (iii) *E. coli* O157:H7 + *Salmonella typhimurium*, (iv) *Staphylococcus aureus* + *E. coli* O157:H7 + *Salmonella typhimurium*. The concentration of each pathogen is 10^5 CFU. (b) LOD test for the detection of three target pathogens on a PMMS-CE microdevice. The concentration of each pathogen is 1, 2, 5, and 10 CFU. The peaks indicate the presence of *Staphylococcus aureus*, *E. coli* O157:H7, and *Salmonella typhimurium* in order.

length control of DNA barcode for each target pathogen and the design of the optimal CE channel.

Limit of detection (LOD) test

Detection limit of pathogen is an important issue in biosafety screening and early diagnosis in biomedical clinics, and the capability of pathogen detection with low cell numbers can eliminate tedious and time-consuming culturing steps. We performed the LOD test for the triplex pathogen detection in the PMMS-CE microdevice by using the three target pathogens and all the particle probes. The input cell number was controlled to be 1, 2, 5, and 10 CFU, and the resultant electropherogram is shown in Fig. 4(b). Even at ultra-low concentration of input cells, all the peaks corresponding to each target pathogen were successfully observed. Note that the multiple fluorescence peak signals at the single-cell level were clearly distinguished from the background signal, allowing the multiplex single cell pathogen detection in the developed PMMS-CE microdevice. The average signal to noise ratios of each target were 19.7 ± 3.05, 28.4 ± 3.81, and 4.3 ± 1.87 for *Staphylococcus aureus*, *E. coli* O157:H7, and *Salmonella typhimurium*, respectively. The large number of barcode DNA strands on each AuNP (*i.e.*, 1.11×10^4, 1.13×10^4, and 1.31×10^4 for *Staphylococcus aureus*, *E. coli* O157:H7, and *Salmonella typhimurium*, respectively) is enough to be detected on the CE microdevice with combination of a laser induced fluorescence detection system.

Conclusions

We have demonstrated highly sensitive, rapid, and multiplex pathogen detection on a novel PMMS-CE microdevice. The sequential processes of pathogen sample-particle probes mixing, magnetic separation, and barcode DNA analysis on a CE device can be completed within 30 min on a chip. The three pathogens are selectively identified even at the single cell level. Such an advanced but simplified integrated PMMS-CE device enables us to perform on-site diagnosis of pathogens from clinical and environmental samples with sample-in-answer-out capability.

Acknowledgements

This work was supported by the R&D Program of MKE/KEIT [10035638, Integrated portable genetic analysis RT-PCR microsystem for ultrafast respiratory infection disease identification], by Technology Development Program for Agriculture and Forestry, Ministry for Agriculture, Forestry and Fisheries, Republic of Korea, and by Basic Science Research Program through the National Research Foundation of Korea (NRF) funded by the Ministry of Education, Science and Technology (2008–0060721).

Notes and references

1 E. Verpoorte, *Electrophoresis*, 2002, **23**, 677–712.
2 V. Srinivasan, V. K. Pamula and R. B. Fair, *Anal. Chim. Acta*, 2004, **507**, 145–150.
3 S. K. Sia, V. Linder, B. A. Parviz, A. Siegel and G. M. Whitesides, *Angew. Chem., Int. Ed.*, 2004, **43**, 498–502.
4 T. M. Squires and S. R. Quake, *Rev. Mod. Phys.*, 2005, **77**, 977–1026.
5 K. E. Jones, N. G. Patel, M. A. Levy, A. Storeygard, D. Balk, J. L. Gittleman and P. Daszak, *Nature*, 2008, **451**, 990–993.
6 H. Zhanga, T. Xua, C.-W. Li and M. Yanga, *Biosens. Bioelectron.*, 2010, **25**, 2402–2407.
7 R. H. Liu, J. Yang, R. Lenigk, J. Bonanno and P. Grodzinski, *Anal. Chem.*, 2004, **76**, 1824–1831.
8 E. T. Lagally, J. R. Scherer, R. G. Blazej, N. M. Toriello, B. A. Diep, M. Ramchandani, G. F. Sensabaugh, L. W. Riley and R. A. Mathies, *Anal. Chem.*, 2004, **76**, 3162–3170.
9 N. Beyor, L. Yi, T. S. Seo and R. A. Mathies, *Anal. Chem.*, 2009, **81**, 3523–3528.
10 P. Liu, T. S. Seo, N. Beyor, K.-J. Shin, J. R. Scherer and R. A. Mathies, *Anal. Chem.*, 2007, **79**, 1881–1889.
11 R. G. Blazej, P. Kumaresan and R. A. Mathies, *Proc. Natl. Acad. Sci. U. S. A.*, 2006, **103**, 7240–7245.
12 P. Ertl, C. A. Emrich, P. Singhal and R. A. Mathies, *Anal. Chem.*, 2004, **76**, 3749–3755.
13 M. Herrmann, T. Veresb and M. Tabrizian, *Lab Chip*, 2006, **6**, 555–560.
14 L. Yu, C. M. Li, Y. Liu, J. Gao, W. Wang and Y. Gan, *Lab Chip*, 2009, **9**, 1243–1247.
15 G. MacBeath, *Nat. Genet.*, 2002, **32**, 526–532.
16 P. Angenendt, J. Glokler, Z. Konthur, H. Lehrach and D. J. Cahill, *Anal. Chem.*, 2003, **75**, 4368–4372.
17 J. C. Paton and A. W. Paton, *Clin. Microbiol. Rev.*, 1998, **11**, 450–479.
18 J.-M. Nam, C. S. Thaxton and C. A. Mirkin, *Science*, 2003, **301**, 1884–1886.
19 S. I. Stoeva, J.-S. Lee, J. E. Smith, S. T. Rosen and C. A. Mirkin, *J. Am. Chem. Soc.*, 2006, **128**, 8378–8379.
20 H. D. Hill and C. A. Mirkin, *Nat. Protoc.*, 2006, **1**, 324–336.
21 E. D. Goluch, J.-M. Nam, D. G. Georganopoulou, T. N. Chiesl, K. A. Shaikh, K. S. Ryu, A. E. Barron, C. A. Mirkin and C. Liu, *Lab Chip*, 2006, **6**, 1293–1299.
22 C. S. Thaxton, H. D. Hill, D. G. Georganopoulou, S. I. Stoeva and C. A. Mirkin, *Anal. Chem.*, 2005, **77**, 8174–8178.
23 J.-M. Nam, K.-J. Jang and J. T. Groves, *Nat. Protoc.*, 2007, **2**, 1438–1444.
24 M. He, K. Li, J. Xiao and Y. Zhou, *J. Virol. Methods*, 2008, **151**, 126–131.
25 X. Zhang, H. Su, S. Bi, S. Li and S. Zhang, *Biosens. Bioelectron.*, 2009, **24**, 2730–2734.
26 B.-K. Oh, J.-M. Nam, S. W. Lee and C. A. Mirkin, *Small*, 2006, **2**, 103–108.
27 S. J. Kim, S. J. Choi, R. Neelamegam and T. S. Seo, *BioChip J.*, 2010, **4**, 42–48.
28 S. J. Kim, G. W. Shin, S. J. Choi, H. S. Hwang, G. Y. Jung and T. S. Seo, *Electrophoresis*, 2010, **311**, 1108–1115.
29 Y. Chen, J. Y. Choi, S. J. Choi and T. S. Seo, *Electrophoresis*, 2010, **311**, 2974–2980.
30 A. D. Stroock, S. K. W. Dertinger, A. Ajdari, I. Mezic, H. A. Stone and G. M. Whitesides, *Science*, 2002, **295**, 647–651.
31 C.-C. Hong, J.-W. Choi and C. H. Ahn, *Lab Chip*, 2004, **4**, 109–113.
32 M. Yi and H. H. Bau, *Int. J. Heat Fluid Flow*, 2003, **24**, 645–656.
33 G. D. Chen, C. J. Alberts, W. Rodriguez and M. Toner, *Anal. Chem.*, 2010, **82**, 723–728.
34 Y. Yamaguchi, F. Takagi, K. Yamashita, H. Nakamura, H. Maeda, K. Sotowa, K. Kisakabe, Y. Yamasaki and S. Morooka, *AIChE J.*, 2004, **50**, 1530–1535.

